Supporting Information

1. **Models of hybrid incompatibility**
   a. **Fig. S1.** Evolution of two-locus BDM incompatibility and fitness of hybrid genotypes.
   b. **Fig. S2.** Evolution of two-locus coevolving incompatibility and fitness of hybrid genotypes.
   c. **Fig. S3.** Fixation of two-locus hybrid incompatibilities under deterministic selection (the Karlin model).
2. **Karlin model with genetic drift (multinomial sampling) and comparison to population simulations.**
   a. **Fig. S4.** Fixation of hybrid incompatibilities under the Karlin model with genetic drift.
   b. **Table S1.** Comparison of rates of fixation for the Karlin model with genetic drift and the simulation program at different population sizes.
3. **Evaluation of the hybrid population reproductive isolation model under a range of parameters**
   a. **Fig. S5.** Probability of isolation with increasing selection on hybrids.
   b. **Table S2.** The effect of increasing selection on hybrids on the probability of and time to isolation.
   c. **Table S3.** The effect of population size on the probability of and time to isolation.
   d. **Fig. S6.** The effect of initial admixture proportion on the probability of isolation.
   e. **Table S4.** Effects of asymmetry in selection on the probability of isolation.
   f. **Table S5**. The effect of variation in dominance.
4. **Incompatibilities that do not result in reproductive isolation in the absence of strong drift.**
   a. **Fig. S7.** Hybrid incompatibility models that do not result in reproductive isolation between hybrid and parental populations in the absence of drift.
   b. **Fig. S8.** The effect of population size on the probability of isolation due to neutral BDM incompatibilities.
5. **Validation of the model under a range of genetic architectures**
   a. **Fig. S9.** Linkage between incompatibility pairs.
   b. **Table S6.** Effect of linkage between hybrid incompatibilities on the probability of and time to isolation.
   c. **Fig. S10.** Mating with parents reduces fitness of hybrid populations after selection.
6. **Validation of the model with a range of demographic scenarios**
   a. **Fig. S11.** Hybrid zone structure used in simulations.
   b. **Table S7.** The effect of on-going and bursts of parental immigration on the probability of and time to isolation.
   c. **Fig. S12.** Structure of multiple hybrid populations.
   d. **Table S8.** Independently formed hybrid populations can evolve reproductive isolation from each other.
   e. **Table S9.** Parental preferences for conspecifics reduce the frequency of hybrid reproductive isolation.

1. Models of hybrid incompatibility

In order to investigate changes in allele frequencies at hybrid incompatibility loci, we need to define explicit models of selection on each two-locus genotype. Different genotypes at hybrid incompatibility loci will experience different strengths of selection. This can be a consequence of dominance at each locus (h), the number of epistatic interactions, the order in which mutations occurred, and the relative fitness of the parental and ancestral genotypes.

Our simulations are based on fitness matrices representing adaptive BDM incompatibilities (Fig. S1) and coevolving hybrid incompatibilities (Fig. S2). Elsewhere, we discuss neutral BDM incompatibilities and coevolving hybrid incompatibilities that will not generate isolation in the absence of strong genetic drift (Fig. S7). For simplicity, in most cases we simulate coevolving incompatibilities (Fig. S2) and assume that selection on different epistatic interactions is symmetrical (s_1=s_2) and that all alleles are codominant (h=0.5). However, we relax these assumptions in Supporting Information 3C and D. Though we focus on coevolving incompatibilities (Fig. S2) our results also generally apply to adaptive BDM incompatibilities (Fig. S1) which have a similar fitness matrix.

In Figures S1A and S2A, we show a single mutational path to each hybrid incompatibility type; however, in both cases, several possible mutational paths exist. Because the lineage and order in which mutations occur is expected to be random (1), we randomly assign a fitness matrix to each incompatibility in simulations (note: these matrices are identical at h=0.5 and s_1=s_2).

Using these fitness matrices and Karlin's two-locus selection model (see Methods, (2)), we can determine the expected trajectory of incompatibility pairs in hybrid populations under

different parameters (Fig. S3). However, some of these dynamics differ in finite populations (see next section).

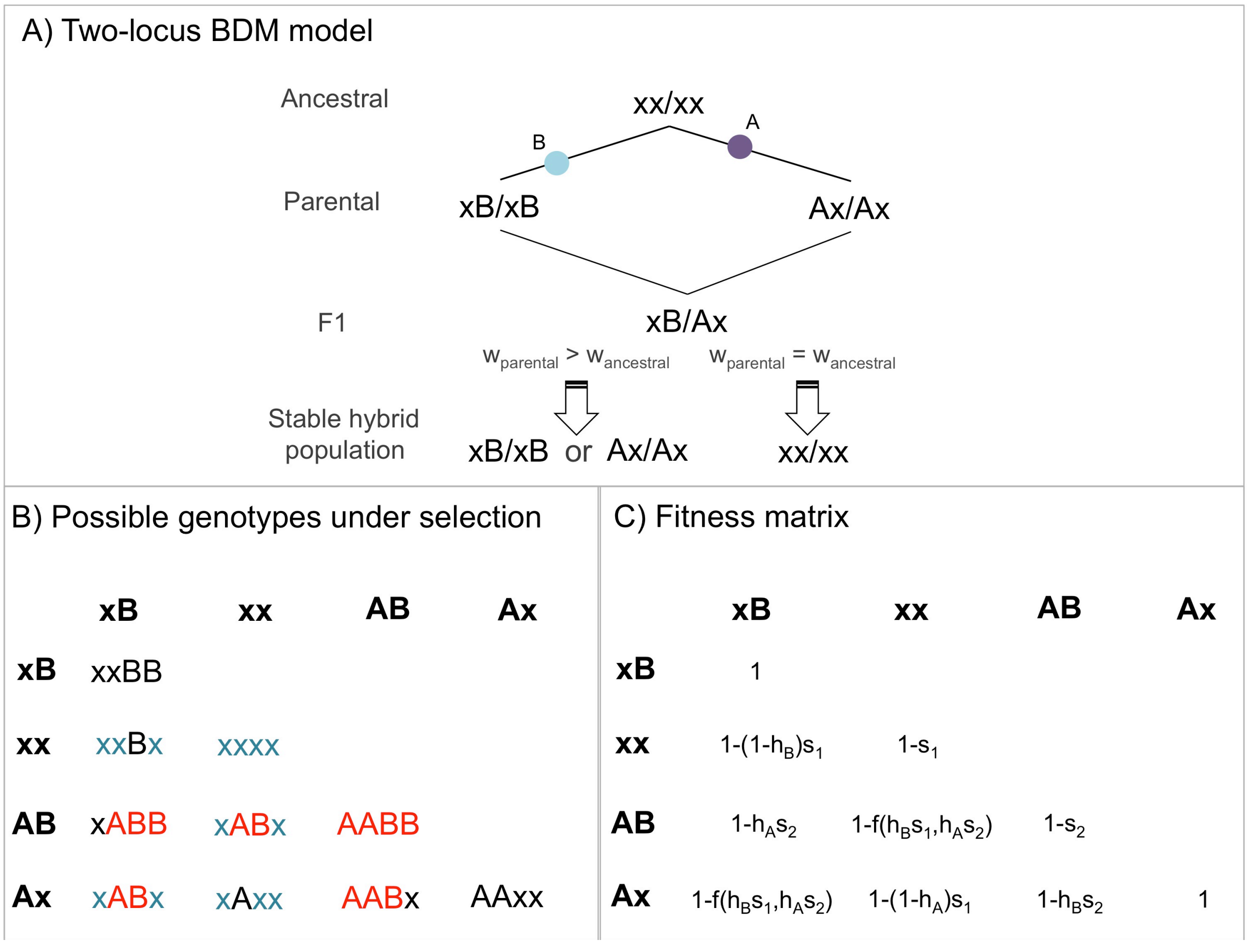

Fig. S1. **Evolution of two-locus BDM incompatibility and fitness of hybrid genotypes.** (A) One of two possible mutational paths to the development of a two-locus BDM incompatibility (Not shown is the case where both mutations occur on one lineage). These incompatibilities can arise as the result of neutral fixation ($w_{parental}=w_{ancestral}$) or as the result of adaptive evolution ($w_{parental}>w_{ancestral}$). (B) Potential selection patterns on hybrid genotypes between the two parentals (assuming $w_{parental}>w_{ancestral}$); genotypes corresponding to selection coefficients s_1 and s_2 are indicated in blue and red respectively. For BDM incompatibilities, s_1 and s_2 can be asymmetric, and in neutral BDM incompatibilities either s_1 or s_2 will equal zero. (C) Fitness of hybrid individuals with each genotype will depend the intensity of selection (s_1, s_2) and dominance (h_A, h_B) at the two loci. We assume, for simplicity that the fitness advantage of all derived genotypes (here, xB and Ax) is equal.

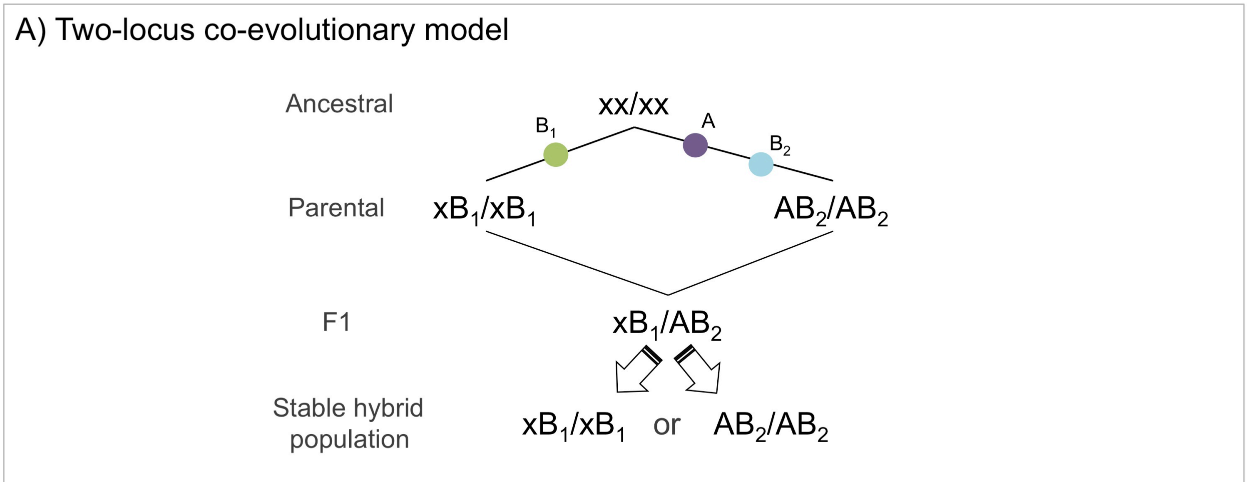

B) Possible epistatic interactions

	xB_1	xB_2	AB_1	AB_2
xB_1	xxB_1B_1			
xB_2	xxB_2B_1	xxB_2B_2		
AB_1	xAB_1B_1	xAB_2B_1	AAB_1B_1	
AB_2	xAB_2B_1	xAB_2B_2	AAB_2B_1	AAB_2B_2

C) Fitness matrix

	xB_1	xB_2	AB_1	AB_2
xB_1	1			
xB_2	$1-(1-h_{B_1})s_1$	$1-s_1$		
AB_1	$1-h_As_2$	$1-f(h_A,h_{B_1},s_1,s_2)$	$1-s_2$	
AB_2	$1-f(h_A,h_{B_1},s_1,s_2)$	$1-(1-h_A)s_1$	$1-h_{B_1}s_2$	1

Fig. S2. **Evolution of two-locus coevolving incompatibility and fitness of hybrid genotypes. (**A) One of two possible mutational paths to the development of a two-locus coevolved incompatibility. Not shown is the case where B_2 precedes A (see Supplement 4). (B) Potential epistatic interactions among hybrid genotypes. Incompatibilities corresponding to s_1 and s_2 are indicated in blue and red, respectively. (C) Fitness of hybrid individuals with each genotype will depend the intensity of selection (s_1, s_2) and dominance (h_A, h_B) at the two loci.

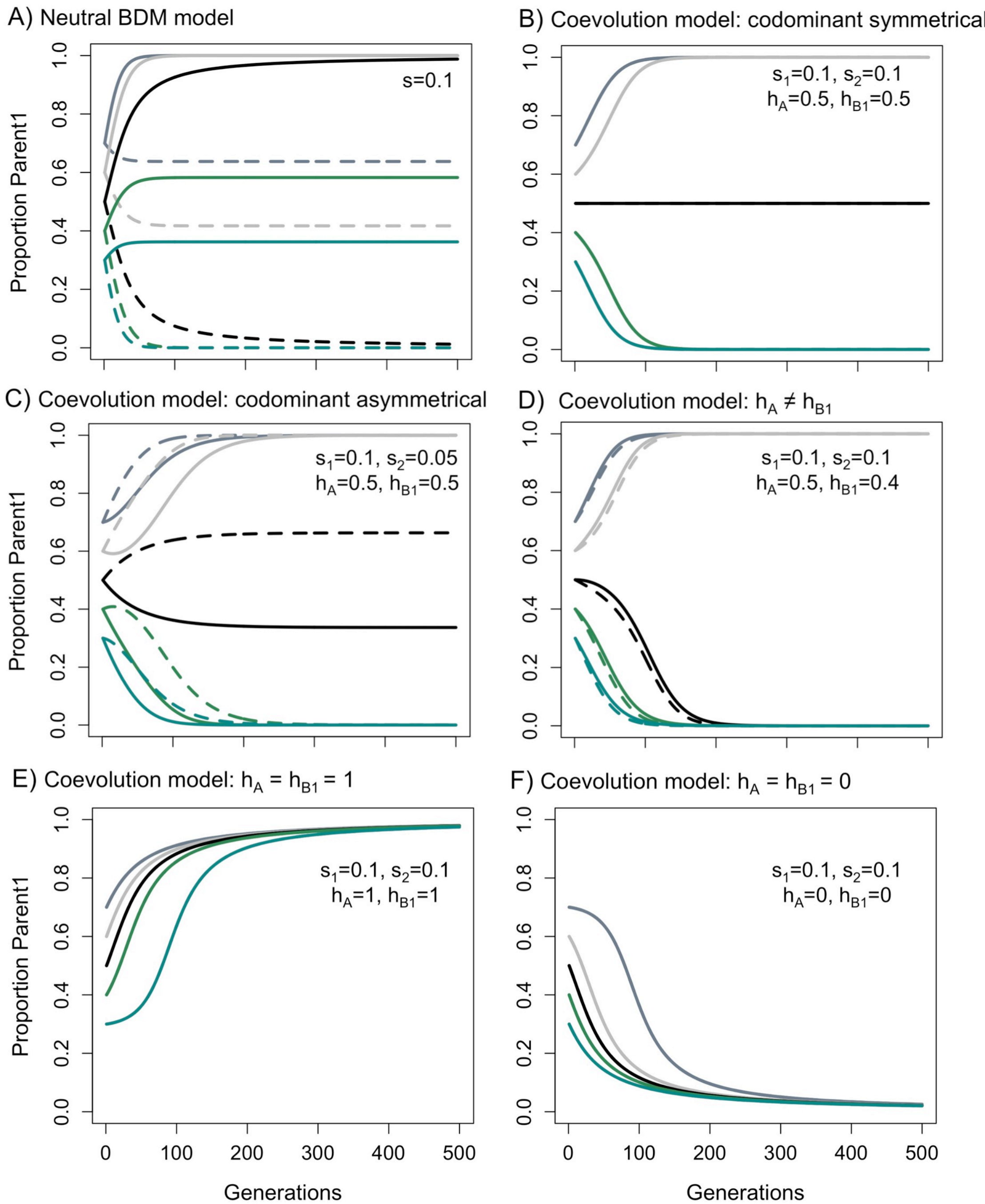

Fig. S3. Fixation of two-locus hybrid incompatibilities under deterministic selection (the Karlin model). The expected parent 1-derived allele trajectories for two unlinked hybrid incompatibilities under the Karlin model depend on starting admixture proportions (*f*=0.3-0.7 shown here), dominance parameters (*h*), and the intensity of selection (i.e. s_1, s_2, see Figs. S1 and S2). The solid line tracks ancestry at locus 1 and the dashed line shows ancestry at locus 2. (A) Neutral BDM incompatibility pairs do not fix if $f \neq 0.5$; at $f = 0.5$ they fix for a hybrid genotype pair that is not incompatible with either parental species (see Supporting Information 4). When incompatibilities are codominant (B, C), the two incompatibility loci fix deterministically for the major parent. At certain values of *h* (D, E, F), fixation is less dependent on initial admixture proportions.

2. Karlin model with genetic drift (multinomial sampling) and comparison to population simulations.

The Karlin model (ref. (2); see Methods) allows us to predict the patterns of fixation for different incompatibility types with different parameters (Fig. S3) but is not realistic because even large populations will have some genetic drift, which is not accounted for in the model. To implement drift, we added multinomial sampling of N individuals at each generation (Fig. S4). The major difference caused by implementing drift is that fixation patterns do not always follow the predictions of the Karlin model. This can be seen most clearly in Fig. S4C, where some fixation trajectories differ from expectations under the Karlin model.

The Karlin equations do not allow us to model the fates of more than one incompatibility pair. We thus wrote an explicit population simulation code (`admix'em`) described in the Methods. To validate this code, we compared results from simulations with `admix'em` to simulations of Karlin's model with drift implemented by multinomial sampling. We simulated a single coevolving hybrid incompatibility (h=0.5, s_1=s_2=0.1) with population size N=1,000 and 10,000. In both cases the results from `admix'em` and Karlin's model with drift are nearly identical (Table S1).

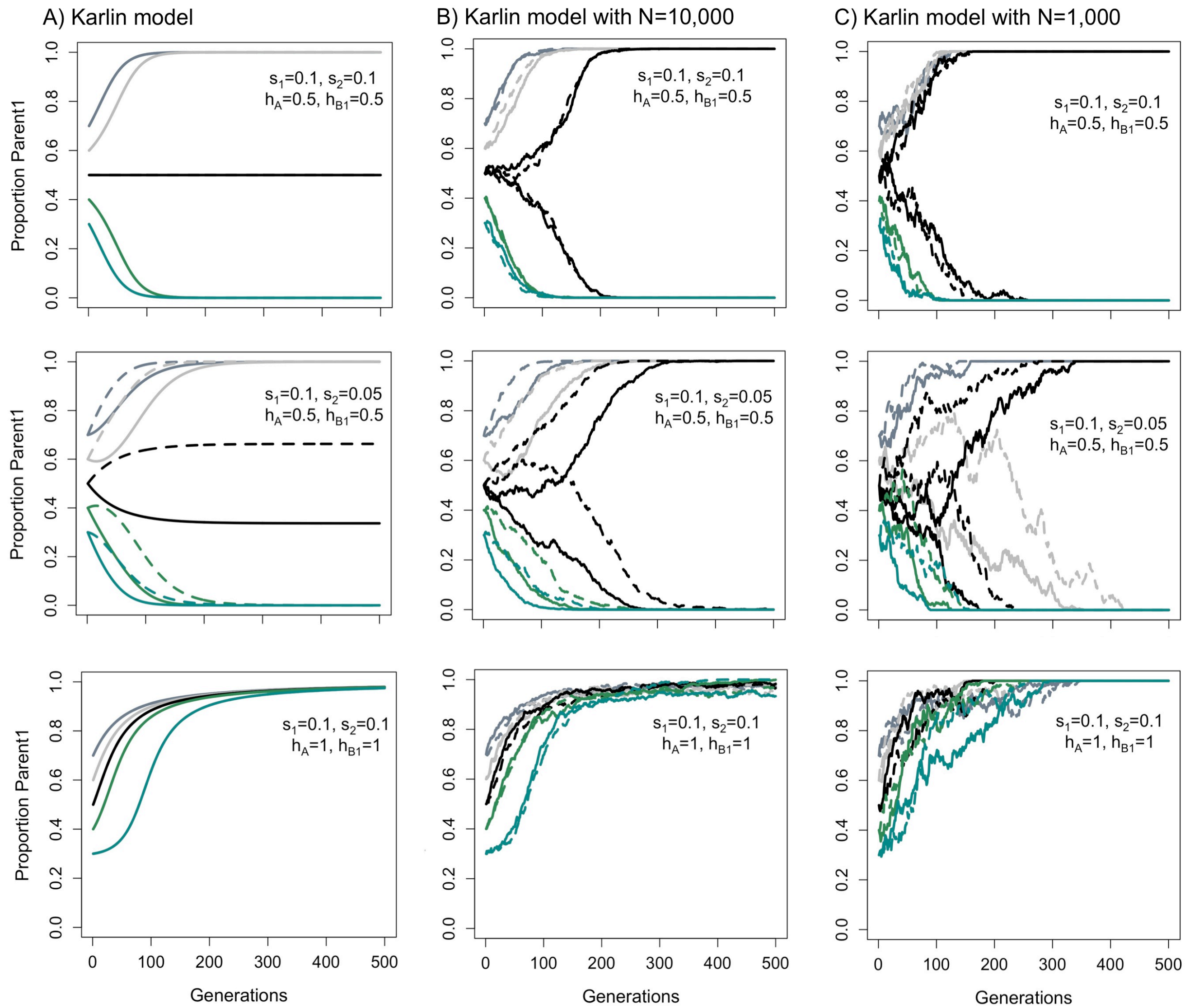

Fig. S4. Fixation of hybrid incompatibilities under the Karlin model with genetic drift. The expected patterns of fixation for a coevolving hybrid incompatibility (Fig. S2) under Karlin's model depend on starting admixture proportions (*f*=0.3-0.7 shown here), dominance parameters (*h*), and asymmetry in selection ($s_1 \neq s_2$). The solid line shows ancestry at locus 1 of an incompatibility and the dashed line shows ancestry at locus 2 of an incompatibility. (A) Parent 1 allele trajectories predicted by the Karlin model for a given set of parameters. (B) Results for the same parameters incorporating multinomial sampling of 10,000 individuals at each generation. (C) Results for the same parameters incorporating multinomial sampling of 1,000 individuals at each generation. Patterns of fixation depend less on initial admixture proportions as drift increases. The equilibrium at *f*=0.5 in the selection-only model is unstable in the presence of drift.

Table S1. Comparison of rates of fixation based on the Karlin model with genetic drift and the `admix'em` simulation program at different population sizes.

	Karlin model with multinomial sampling		admix'em	
Diploid population size (N)	Percent fixing parent 1 genotype ± SE	Average time to fixation ± SD	Percent fixing parent 1 genotype ± SE	Average time to fixation ± SD
1,000	49.8 ± 2	152 ± 42	50.2 ± 2	154 ± 40
10,000	50.6 ± 2	201 ± 44	51.0 ± 2	193 ± 32

Note – One hybrid incompatibility pair (Fig. S2), s_1=s_2=0.1, f=0.5, h=0.5 for 500 replicate simulations.

3. Evaluation of the hybrid population reproductive isolation model under a range of parameters

Simulations presented in the main text demonstrate that with two hybrid incompatibility pairs, reproductive isolation frequently evolves (47±2%) due to fixation of hybrid incompatibility loci for both parents. This mechanism of hybrid isolation is most likely to be biologically relevant if it occurs under a broad range of parameters. We performed simulations of two coevolving hybrid incompatibility pairs (Fig. S2) varying selection (s), dominance (h), diploid population size (N), admixture proportions (f), and degree of asymmetry in selection ($s_1 \neq s_2$). All results are based on 500 replicate simulations. We consider hybrid populations "isolated" from both parents if they fix for at least one incompatibility pair from each parent; the strength of isolation will always depend on the strength of selection on each incompatibility and the number of incompatibilities. Together, these simulations demonstrate that hybrid reproductive isolation due to fixation of genetic incompatibilities can occur under a range of parameters.

A. The strength of selection on hybrids.

Variation in the strength of selection on hybrids can influence the likelihood of hybrid isolation under our model. We performed simulations with two coevolving hybrid incompatibility pairs with different strengths of selection (Table S2, Fig. S5). We find that the probability of isolation decreases as total selection on hybrids increases. Lower probability of isolation at higher levels of selection on hybrids is the result of hybrid populations becoming dominated by parental individuals.

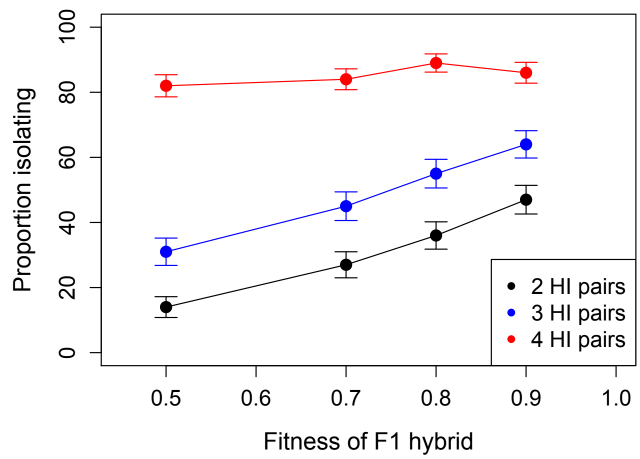

Fig. S5. Probability of isolation with increasing selection on hybrids. With increasing selection on F_1 hybrids between the parental species, the probability that hybrid populations will develop reproductive isolation from both parents decreases. This result is less pronounced with a greater number of hybrid incompatibility (HI) pairs. Error bars show two standard deviations. Simulation parameters were h=0.5, s_1=s_2, f=0.5, and N=1,000.

Table S2. The effect of increasing selection on hybrids on the probability of and time to isolation.

Fitness of F1 hybrid	Percent isolating ± SE	Average time to isolation ± SD
0.9	47 ± 2	150 ± 48
0.8	36 ± 2	78 ± 21
0.7	27 ± 2	55 ± 14
0.5	14 ± 2	53 ± 9

Note – Two hybrid incompatibility pairs (Fig. S2), s_1=s_2, N=1000, f=0.5, h=0.5 for 500 replicate simulations.

B. Population size

A number of models of speciation rely on small population sizes to achieve isolation from parental species (e.g. see (3, 4)). One feature of our model is that it does not rely on small population sizes; in large populations incompatibility pairs fix by selection, whereas in small populations they fix by chance. As a result, the proportion of hybrid populations evolving isolation from both parents is not strongly dependent on population size (Table S3). This suggests that our model is applicable to a range of natural hybrid populations.

Table S3. The effect of population size on the probability of and time to isolation.

Diploid population size (N)	**Percent isolating ± SE**	**Average time to isolation ± SD**
100	40 ± 2	75 ± 34
1000	47 ± 2	150 ± 48
10000	44 ± 2	190 ± 43

Note – Two hybrid incompatibility pairs (Fig. S2), s_1=s_2=0.1, f=0.5, h=0.5 for 500 replicate simulations.

C. Initial admixture proportions

To determine how changing admixture proportions influences the number of hybrid populations evolving isolation, we varied starting admixture proportions from f=0.5-0.7. As expected, the probability of isolation from both parents decreased with increasing ancestry skew (Fig. S6). Initial admixture proportions close f=0.5 are most likely to result in isolation from both parental species. However, even in skewed populations, isolation from both parents was possible when assuming variation in dominance among alleles (for e.g. h =Uniform(0,1), Fig. S6) or at lower population sizes (N=100, Fig. S6).

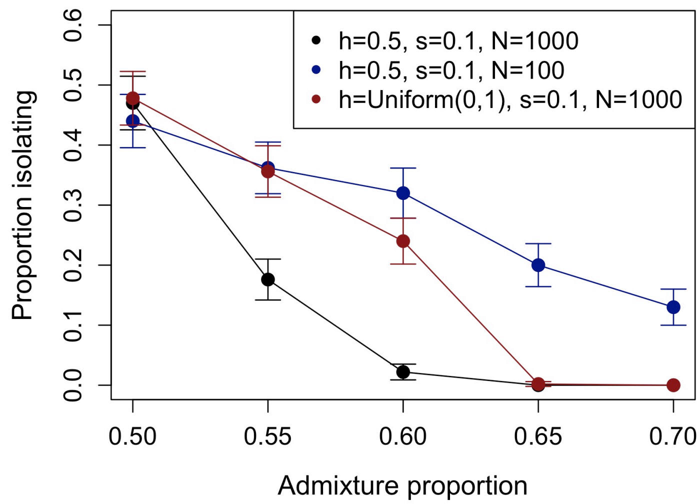

Fig. S6. The effect of initial admixture proportion on the probability of isolation. Proportion of hybrid populations developing isolation from both parents as a function admixture proportions, dominance (*h*) and population size (two incompatibility pairs, *s*1=*s*2=0.1). Isolation occurs most frequently at equal admixture proportions, but can occur in ancestry-skewed populations, especially if the populations are small or there is variation in dominance. Error bars show two standard deviations.

D. Asymmetric selection on hybrid incompatibilities

For simplicity, in most cases we simulate symmetric selection on hybrid incompatibilities. To introduce asymmetric selection on different hybrid genotypes we use different selection coefficients for distinct interactions in the coevolution model, s_1 and s_2 (Fig. S2). When selection is asymmetrical (i.e. $s_1 \neq s_2$), the Karlin model has similar properties to $s_1 = s_2$ as long as s_1 and s_2 are both greater than 0 (Fig. S3). To investigate this in finite populations, we randomly assigned s=0.1 to s_1 or s_2 independently for two coevolving incompatibility pairs and set the value for the other selection coefficient to 0.2*s, 0.3*s, 0.4*s, or 0.5*s. In these simulations, reciprocal isolation still developed frequently (Table S4).

The adaptive BDM model (Fig. S1) might result in even more extreme asymmetry in selection on hybrid genotypes (5-7). To approximate this scenario, we simulated adaptive BDMIs (Fig. S1) and randomly assigned s=0.5 to s_1 or s_2 independently for two hybrid incompatibility pairs, and assigned s=0.02 to the other selection coefficient. In these simulations 39 ± 2% of populations became isolated from both parental species. In populations fixing incompatibility pairs from both parents, the strength of isolation from each parent species was similar. On average, the absolute fitness difference between backcross types (hybrid x parent 1 and hybrid x parent 2) was only 0.003. The average fitness of a hybrid x parent cross after hybrid populations fixed for parental incompatibilities was 0.87 (compared to 0.76 for an F1 cross between the two parent species).

Table S4. Effects of asymmetry in selection on the probability of isolation.

Asymmetry of selection	Percent isolating ± SE	Average time to isolation ± SD
s_A=s_B	47 ± 2	150 ± 48
s_A=0.5*s_B	44 ± 2	211 ± 64
s_A=0.4*s_B	46 ± 2	232 ± 73
s_A=0.3*s_B	44 ± 2	290 ± 86
s_A=0.2*s_B	36 ± 2	319 ± 85
s_A=0*s_B	0.2 ± 0.2	497 (NA)

Note – Two hybrid incompatibility pairs (Fig. S1, S2), s_A=0.1, N=1000, f=0.5, h=0.5 for 500 replicate simulations.

E. Dominance

In the above simulations, we model codominant hybrid incompatibilities but varying dominance (h) does not have major effects on our conclusions. To demonstrate this, we simulated two scenarios: 1) we drew h from a uniform distribution, requiring h at each locus to add to 1 and 2) we randomly assigned h discrete values of 0 (recessive), 0.5 (co-dominant), or 1 (dominant), again requiring h to add to 1 at each locus. Both of these scenarios result in a similar probability of isolation from parental species (Table S5).

Table S5. The effect of variation in dominance.

Dominance	**Percent isolating ± SE**	**Average time to isolation ± SD**
$h = 0.5$	47 ± 2	150 ± 48
h = Uniform(0,1)	48 ± 2	120 ± 36
$h \in (0, 0.5, 1)$	44 ± 2	118 ± 37

Note – Two hybrid incompatibility pairs (Fig. S2), s_1=s_2=0.1, N=1000, f=0.5, for 500 replicate simulations.

4. Incompatibilities that do not frequently result in reproductive isolation in the absence of strong drift

Several types of genetic incompatibilities, such as neutral BDM incompatibilities (or other scenarios that generate identical fitness matrices, Fig. S7), are not predicted to contribute to reproductive isolation between hybrids and parentals by incompatibility selection (Fig. S7). This is because hybrid incompatibility pairs either do not fix, or fix for a genotype that is compatible with both parents (based on the Karlin model, Fig. S3A, Fig. S7). Simulations of incompatibilities with these fitness matrices confirm this prediction; the most frequently fixed genotype is not incompatible with either parent (54±2% of simulations) and in many simulations (45±2%) hybrid populations did not fix for a particular parental genotype at incompatibility loci within 2,000 generations (simulation parameters: N=1000, s=0.1, f=0.5, h=0.5).

Nonetheless, with strong genetic drift, genotypes incompatible with one of the parents can fix by chance, contributing to isolation, even under a neutral BDMI model. This can be seen in Fig. S8, which shows the proportion of hybrid populations isolated from both parents as a function of population size. As population size decreases and drift increases, the proportion of hybrid populations isolating from both parents increases. However, the time to isolation is longer than in cases where fixation is driven by deterministic selection (by drift N=100: 215±105 generations, N=500: 1267±506 generations, N=1000: 1312±278 generations, compared to Table S3).

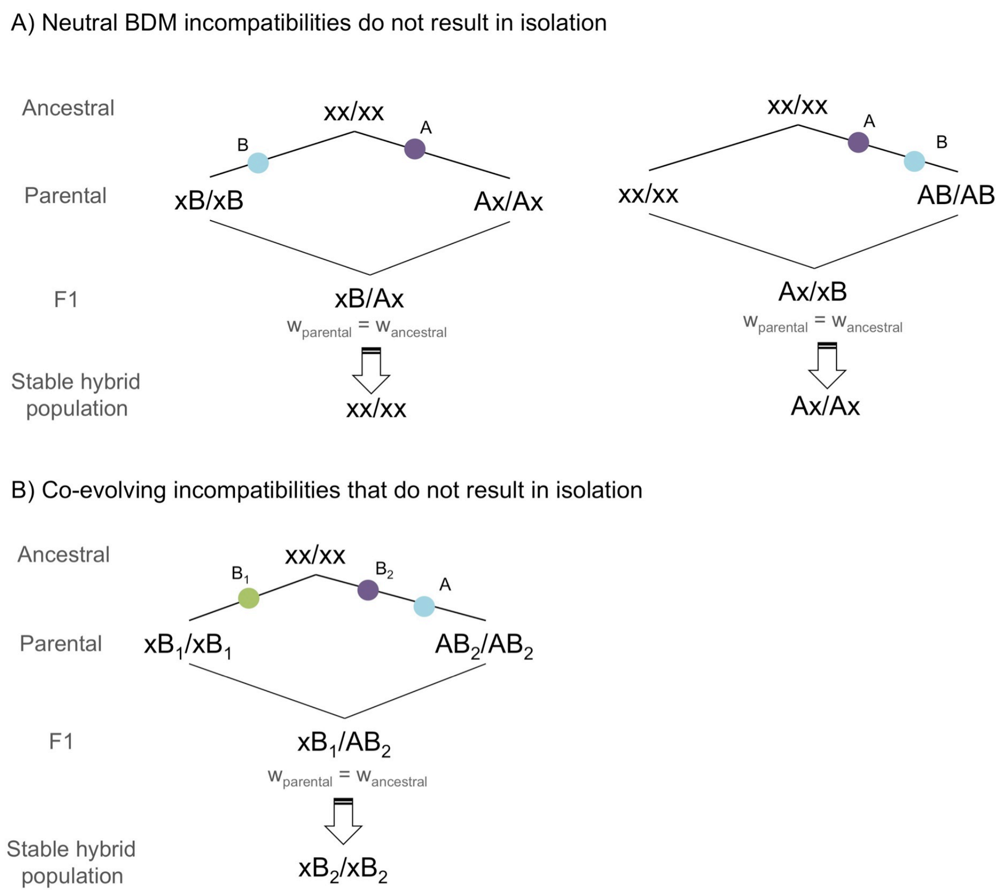

Fig. S7. Hybrid incompatibility models that do not frequently result in reproductive isolation between hybrid and parental populations in the absence of drift. (A) When hybrid populations form at equal admixture proportions, the deterministic model predicts that neutral BDM incompatibilities will fix for the ancestral genotype in a two-lineage model (left) and a genotype that is compatible with both species in a one-lineage model (right). (B) In a coevolution scenario, certain mutation orders result in an identical fitness matrix to A and thus do not result in reproductive isolation in hybrid populations. In all cases depicted, mutations in lineage 1 could occur in lineage 2 and vice versa but the expected effects on isolation from parental species do not change.

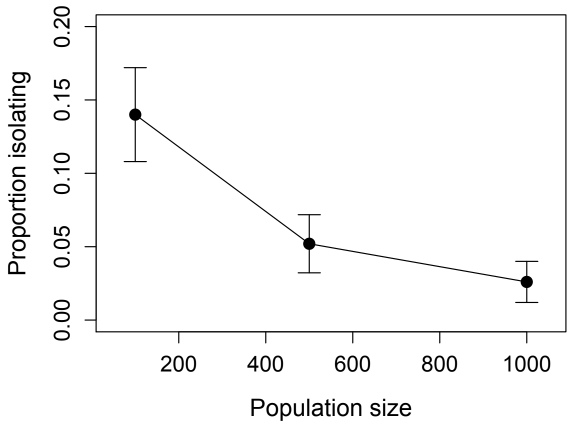

Fig. S8. The effect of population size on the probability of isolation due to neutral BDM incompatibilities. As drift increases, the proportion of hybrid populations isolated from parentals by fixation of neutral BDM incompatibilities increases. However, this process does not occur as rapidly as deterministic selection on other types of hybrid incompatibilities. Simulation parameters: two neutral BDMI pairs (Fig. S7), s=0.1, f=0.5, h=0.5 for 500 replicate simulations.

5. Validation of the model under a range of genetic architectures

Because species are likely to be differentiated by a number of incompatibilities even in the early stages of speciation (8), we investigated how the number of incompatibility pairs and their genetic architecture affects the probability of evolving reproductive isolation.

A. Number of incompatibility pairs

Theoretically, increasing the number of incompatibility pairs should increase the probability that hybrid populations will become isolated from both parents (by at least one incompatibility). However, increasing the number of incompatibility pairs will reduce hybrid fitness and thus may also increase the probability that hybrids will be outcompeted by parental species. Simulating 3-6 unlinked coevolving incompatibility pairs (f=0.5, h=0.5, s_1=s_2=0.1, N=1000) increased the probability of isolation as a function of the number of pairs (Fig. 4, 58-96%). This result is notable because the probability of reciprocal isolation increases even with an increase in total selection on hybrids (see also Fig. S5).

B. Probability of reciprocal isolation in the presence of neutral BDM incompatibilities

Though there is little data on fitness matrices for specific hybrid incompatibilities (reviewed in 9), neutral BDM incompatibilities may be common (1). Because of this, we determined the frequency of isolation between hybrids and parents in simulations including neutral BDM incompatibilities, where either s_1 or s_2 equals zero. We simulate two coevolving hybrid incompatibility pairs as described above but also include one linked or unlinked neutral BDM incompatibility pair. We find that the presence of BDM incompatibilities does not significantly decrease the probability of isolation between hybrid and parental populations

(unlinked: 45 ± 2%, 1 cM between coevolving incompatibility and neutral BDM as in Figure S9B: 48 ± 2%, compared to 47 ± 2% with no neutral BDMIs). Interestingly, linkage between a neutral BDM incompatibility and a coevolving incompatibility can result in more frequent fixation of one of the parental genotypes at BDMIs (21± 2%, compared to 0.2% without linkage). In such cases, neutral BDMIs will contribute to isolation between hybrids and parental species.

C. Linkage between incompatibility pairs

Linkage between sites involved in hybrid incompatibilities could influence the frequency of isolation because ancestry at linked sites will be correlated. In order to investigate this we simulated two coevolving hybrid incompatibility pairs and varied genetic distance between loci (50 cM, 10 cM, and 1 cM, Fig. S9). Some scenarios of physical linkage did not have a strong effect on the probability of isolation, while others reduced the probability of isolation (Table S6).

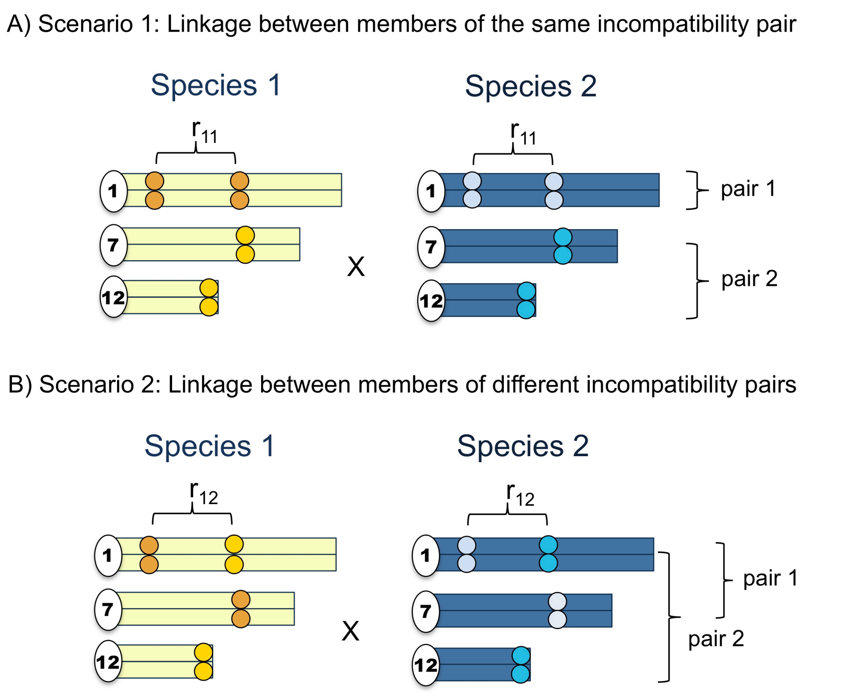

Fig. S9. Linkage between incompatibility pairs. Linkage between incompatibility pairs can change the probability of hybrid populations evolving reproductive isolation (Table S6). (A) In scenario 1, linkage between loci in the same incompatibility pair does not influence the frequency of hybrid populations evolving reproductive isolation. (B) In linkage scenario 2, linkage between loci in different incompatibility pairs significantly decreases the frequency at which hybrid populations evolve reproductive isolation. The probability of recombination between two sites is indicated as *r*.

Table S6. Effect of linkage between hybrid incompatibilities on the probability of and time to isolation.

Linkage scenario (Fig. S9)	Genetic distance	Percent isolating ± SE	Average time to isolation ± SD
Scenario 1	50 cM	47 ± 2	133 ± 35
Scenario 2	50 cM	43 ± 2	137 ± 51
Scenario 1	10 cM	28 ± 2	130 ± 31
Scenario 2	10 cM	43 ± 2	137 ± 35
Scenario 1	1 cM	6 ± 1	157 ± 23
Scenario 2	1 cM	47 ± 2	122 ± 28

Note – A visual representation of the linkage scenarios can be found in Fig. S9. Simulation parameters: Two hybrid incompatibility pairs (Fig. S2), s_1=s_2=0.1. N=1000, f=0.5, h=0.5 for 500 replicate simulations.

D. More complex incompatibility architectures

We have focused on very simple models that show that hybrid reproductive isolation can evolve in principle. However, empirical studies suggest that even closely related species are sometimes differentiated by dozens of incompatibilities that vary in their fitness effects (10-14). To investigate whether hybrid reproductive isolation evolves with more complex incompatibility architectures, we simulated a large number of incompatibilities with variation in selection, dominance, and asymmetry. We simulate 20 pairs of hybrid incompatibilities with a randomly chosen genomic position (chromosome 1-20, position 1-25000000 bp). Dominance is drawn from a uniform distribution (0-1) and selection coefficients (s_1 and s_2) are drawn from an exponential distribution with a mean of s=0.05. Because s_1 and s_2 are determined independently this introduces asymmetry in selection, and if s_1 or s_2 is close to 0 (i.e. on the order of 1/N), this generates an effectively neutral BDM incompatibility.

In these simulations, hybrid populations had a high probability of developing isolation from both parental species (95±1%). On average, backcrosses between parentals and individuals from the hybrid population had a fitness of 0.79±0.11 after 500 generations of selection on hybrid populations, compared to an average of 0.61±0.07 for F_1 hybrids between the two parental species (Figs. 3, S10). The average fitness of hybrids mating with other hybrids in the population was 0.97±0.02.

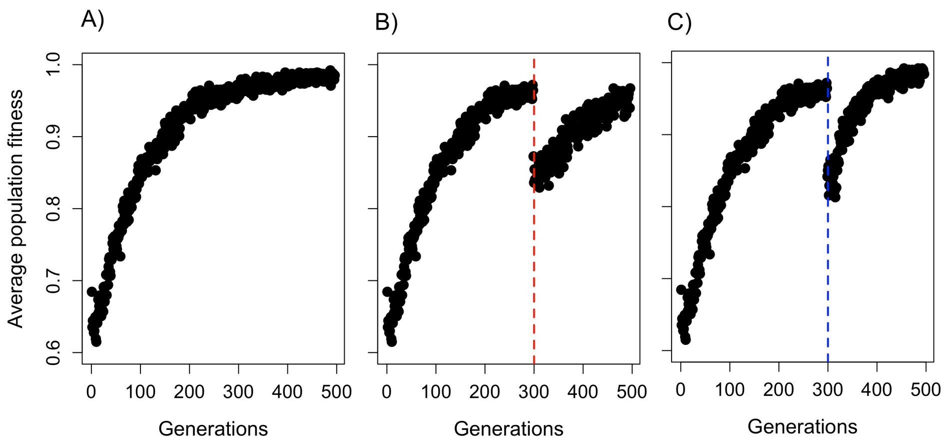

Fig. S10. Mating with parents reduces fitness of allopatrically evolved hybrid populations. (A) Change in average hybrid population fitness over time in a simulation of 20 incompatibility pairs with dominance and selection coefficients drawn from an exponential distribution (see Supporting information 5D). (B) The same hybrid population with a one generation burst of migrants from parent 1 ($4Nm_1$=400) at generation 300. (C) The same hybrid population with a one generation burst of migrants from parent 2 ($4Nm_2$=400) at generation 300. Notably, hybrid populations have lower average fitness after gene flow with either parent, but recover rapidly.

6. Validation of the model under a range of demographic scenarios

A. Isolation with migration

Hybrid populations in nature frequently experience ongoing gene flow with parental species. Given this, it is important to determine the impact of gene flow on how frequently hybrid populations evolve reproductive isolation. We simulated two migration scenarios, one with continuous migration from both parental populations ($4Nm = 8 – 40$) and one with a single pulse of migration from either parent (migrating parent determined randomly) at 25, 50, and 75 generations in independent simulations respectively. Because populations with ongoing migration from both parents never completely fix for a particular genotype, we treated cases in which 95% of the hybrid population had a particular genotype as fixed. As expected, higher migration rates lowered the proportion of hybrid populations evolving isolation from both parents (Table S7, compared to 47± 2% with no migration). However, our results demonstrate that isolation still occurs frequently with fairly high levels of gene flow from the parental species. Notably, even before fixation, pulses of migration from parental populations lower hybrid population fitness (Fig. 3, Fig. S9).

B. Migration in a stepping stone hybrid zone

We use the simplest hybrid zone structure in our simulations (Fig. 1A of the manuscript), but hybrid zones often exist as a series of populations between the parental species. To simulate this, we modeled three hybrid populations between the parental populations with bidirectional migration between adjacent populations (Fig. S11, Table S7). In this scenario, the hybrid population at the center of the hybrid zone (H2, Fig. S11) experiences less direct gene flow from

the parental populations, and should evolve reproductive isolation more frequently at the same migration rate. As expected, we found that the hybrid population at the center of the hybrid zone developed isolation from parental species more frequently (Table S7), but that hybrid populations closer to the parentals were less likely to develop isolation (4*Nm*=8: 26±2 - 30±2%, 4*Nm*=20: 1.6±0.6 - 2.0±0.6%, 4*Nm*=40: 0). This suggests that more realistic hybrid zone structures could actually increase the likelihood that some hybrid populations will evolve reproductive isolation by buffering effective gene flow from parental species.

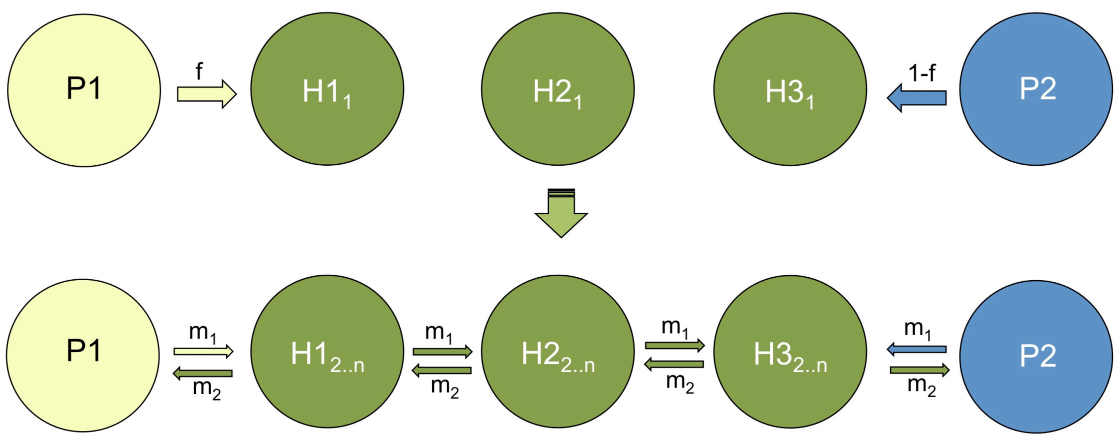

Fig. S11. Hybrid zone structure used in simulations. Model of hybrid zone structure used in simulations of complex hybrid zone structures (see Supporting Information 6B). This structure of a gradient of hybrid populations with ongoing gene flow from parental and other hybrid populations is similar to many naturally occurring hybrid populations.

Table S7. The effect of on-going and bursts of parental immigration on the probability of and time to isolation.

Migration scenario	**Hybrid zone structure**	**Percent isolating ± SE**	**Average time to isolation ± SD**
Continuous (4*Nm*=8)	Fig. 1A	37 ± 2	174 ± 49
Continuous (4*Nm*=20)	Fig. 1A	27 ± 2	247 ± 81
Continuous (4*Nm*=40)	Fig. 1A	0.6 ± 0.3	384 ± 86
Burst – generation 25 (4*Nm*=400)	Fig. 1A	36 ± 2	153 ± 48
Burst – generation 50 (4*Nm*=400)	Fig. 1A	38 ± 2	151 ± 44
Burst – generation 75 (4*Nm*=400)	Fig. 1A	38 ± 2	152 ± 47
Continuous (4*Nm*=8)	Fig. S11	47 ± 2	153 ± 44
Continuous (4*Nm*=20)	Fig. S11	32 ± 2	233 ± 79
Continuous (4*Nm*=40)	Fig. S11	1 ± 0.4	371 ± 130

Note – Two hybrid incompatibility pairs (Fig. S2), s_1=s_2=0.1, N=1000, *f*=0.5, *h*=0.5 for 500 replicate simulations. For the "Burst" models, all migration occurs in one generation.

C. Reciprocal isolation of multiple hybrid populations

One interesting prediction of our model is that independent hybrid populations that form from the same parental species could evolve reproductive isolation from each other, if they fix for different parental alleles at incompatibility pairs. To investigate this, we simulated two hybrid populations formed from the same parental species (Fig. S12). In cases where both hybrid populations in a simulation evolved isolation from the parents, we asked how frequently these populations were isolated from each other. When there was no gene flow between the hybrid populations, isolation evolved frequently between these populations (2 HI: 52 ± 2% 3HI: 80 ± 2%, Table S8). However, when hybrid populations were connected by gene flow, this outcome was significantly less likely (Table S8). These simulations suggest that hybridization between the same parental species could generate multiple, reproductively isolated hybrid populations, but that this outcome is more likely when gene flow is lower.

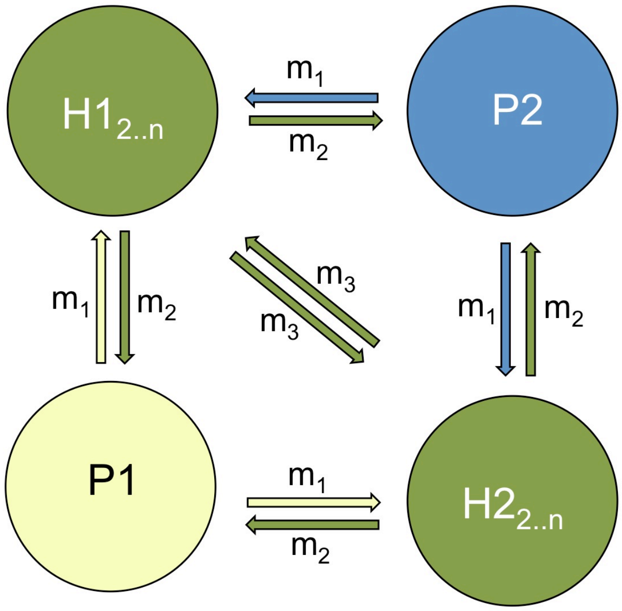

Fig. S12. Structure of multiple hybrid populations. Hybrid zone structure used in simulations of reciprocal hybrid isolation (Supporting Information 6B).

Table S8. Independently formed hybrid populations can evolve reproductive isolation from each other.

Number of incompatibility pairs	Migration rate	Percent reciprocally isolated ± SE
2	$4Nm=0$	52 ± 5
2	$4Nm=8$	18 ± 4
2	$4Nm=20$	0
3	$4Nm=0$	80 ± 4
3	$4Nm=8$	66 ± 5
3	$4Nm=20$	7 ± 3

Note – Two or three hybrid incompatibility pairs (Fig. S2), $s_1=s_2=0.1$, N=1000, $f=0.5$. Simulations conducted until 100 replicates were generated in which both hybrid populations were isolated from parentals.

D. Non-random mating of parents in hybrid zones

In our simulations, mating is random, and pure parental individuals become less common as the number of generations since initial hybridization increases. However, if parentals mate assortatively, larger numbers will exist in the hybrid population, increasing the risk of out-competition of hybrids by parents. To investigate this, we implemented a mating rule in which migrating parentals mate exclusively with conspecifics. If a conspecific is not sampled in 25, 50, or 75 attempts in separate simulations respectively, the parental individual does not mate. With increasing parental effort to mate with a conspecific, hybrid populations evolved isolation less frequently (Table S9). This suggests that hybrid populations are more likely to be outcompeted if parentals have strong preferences against mating with hybrids.

Table S9. Parental preferences for conspecifics reduce the frequency of hybrid reproductive isolation.

Parental preference	Percent isolating ± SE	Average time to isolation ± SD
None	47± 2%	150 ± 48
25 attempts	42 ± 2%	322 ± 85
50 attempts	33 ± 2%	384 ± 79
75 attempts	34 ± 2%	328 ± 74

Note – Two hybrid incompatibility pairs (Fig. S2), $4Nm_1=4Nm_2=8$, $s_1=s_2=0.1$, N=1000, f=0.5, h=0.5 for 500 replicate simulations.

Supporting References

1. Coyne JA & Orr HA (2004) *Speciation* (Sinaeur Associates, Sunderland, MA).
2. Karlin S (1975) General 2-locus selection models - Some objectives, results and interpretations. *Theor Popul Biol* 7(3):364-398.
3. Gavrilets S & Hastings A (1996) Founder effect speciation: A theoretical reassessment. *Am Nat* 147(3):466-491.
4. Grant V (1971) *Plant Speciation* (Columbia University Press, New York).
5. Gavrilets S (1997) Hybrid zones with Dobzhansky-type epistatic selection. *Evolution* 51(4):1027-1035.
6. Unckless RL & Orr HA (2009) Dobzhansky-Muller incompatibilities and adaptation to a shared environment. *Heredity* 102(3):214-217.
7. Johnson NA, Wolf JB, Brodie ED, III, & Wade MJ (2000) Gene interactions and the origin of species. *Epistasis and the evolutionary process.*, eds Wolf J, Brodie EI, & Wade M (Oxford University Press, New York), pp 197-212.
8. Cutter AD (2012) The polymorphic prelude to Bateson-Dobzhansky-Muller incompatibilities. *Trends in Ecology & Evolution* 27(4):209-218.
9. Presgraves DC (2010) The molecular evolutionary basis of species formation. *Nat Rev Genet* 11(3):175-180.
10. Moyle LC & Graham EB (2006) Genome-wide associations between hybrid sterility QTL and marker transmission ratio distortion. *Mol Biol Evol* 23(5):973-980.
11. Harushima Y, Nakagahra M, Yano M, Sasaki T, & Kurata N (2001) A genome-wide survey of reproductive barriers in an intraspecific hybrid. *Genetics* 159(2):883-892.

12. Payseur BA & Hoekstra HE (2005) Signatures of reproductive isolation in patterns of single nucleotide diversity across inbred strains of mice. *Genetics* 171(4):1905-1916.

13. Corbett-Detig RB, Zhou J, Clark AG, Hartl DL, & Ayroles JF (2013) Genetic incompatibilities are widespread within species. *Nature* 504(7478):135-+.

14. Payseur BA, Krenz JG, & Nachman MW (2004) Differential patterns of introgression across the X chromosome in a hybrid zone between two species of house mice. *Evolution* 58(9):2064-2078.